Intramolecularity and the Function of the Side Arm Base of Simple Models of Transaminases

Yikang Wu and Per Ahlberg*

Department of Organic Chemistry, University of Göteborg, S-41296 Göteborg, Sweden

Received April 28, 1992

In the past decade remarkable success[1] has been achieved in designing and synthesizing artificial transaminases. Among these model compounds, many exhibit significantly increased transamination rates due to the presence of a basic catalytic side arm which facilitates the proton transfer in the ketimine–aldimine tautomerization (a key stage in transamination). The function of the side arm base has been investigated with some particular compounds and a generalized conclusion[1a,2,3] that the base plays a dual function (abstracting and then delivering proton intramolecularly) has been drawn. However, the evidence so far available is not unequivocal[4] and further investigation is therefore still necessary.

We have now examined the effect of varying reactant concentration on the transamination rate. The idea is that depending on the predominant mechanism, the variation[5] of the k_{obsd} will differ from compound to compound with respect to a given increase in the reactant concentration. If both steps (deprotonation and reprotonation) of the ketimine–aldimine conversion (Figure 1) are accomplished intramolecularly, the k_{obsd} will not increase with the increase of the reactant concentration.

In order to explore the influence of the chain length on the function of the side arm base while not causing significant misleading interference due to the structural alterations, a special set of model compounds[7] (which are closely related to each other, with the side arm length as essentially the only difference, Figure 2) was chosen for the present work. The transamination rate of each compound was determined at three concentration levels (Table I).

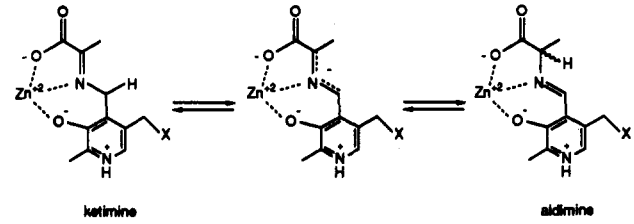

Figure 1. A simplified representation of the ketimine–aldimine tautomerization in the presence of Zn^{2+}. For clarity the base which carries out the proton transfer is not shown.

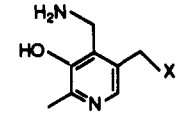

Cmpd	n	X	Cmpd	n	X
1	0	OH	4	4	$S(CH_2)_2NMe_2$
2	1	NMe_2	5	5	$S(CH_2)_3NMe_2$
3	3	$(CH_2)_2NMe_2$	6	6	$S(CH_2)_4NMe_2$

Figure 2. The compounds used in the present work.

Table I.[a] The Pseudo-First-Order Rate Constants for the Ketimine–Aldimine Conversion (Figure 1) at Different Concentrations

n	compd	k_a/s^{-1} (0.08 mM)	k_b/s^{-1} (0.16 mM)	k_c/s^{-1} (0.32 mM)	k_b/k_a	k_c/k_a
0	1	9.4×10^{-6}	1.8×10^{-5}	2.2×10^{-5}	1.90	2.30
1	2	7.4×10^{-5}	1.3×10^{-4}	2.0×10^{-4}	1.80	2.70
3	3	3.5×10^{-4}	5.7 ± 10^{-4}	8.4×10^{-4}	1.60	2.40
4	4	2.4×10^{-4}	2.6×10^{-4}	3.0×10^{-4}	1.10	1.30
5	5	8.2×10^{-4}	6.7×10^{-4}	5.0×10^{-4}	0.82	0.61
6	6	1.6×10^{-4}	1.3×10^{-4}	1.3×10^{-4}	0.81	0.81

[a] All runs were carried out in MeOH at "pH 4.0" (as read with a glass electrode) at 30.0 °C with a constant molar ratio of 1:10:1 (model compound/pyruvic acid/$Zn(OAc)_2 \cdot 2H_2O$). k_a, k_b, and k_c are the k_{obsd} at 0.08, 0.16, and 0.32 mM, respectively (ref 6). The standard deviations for all runs were <1% with duplicate runs within 10%. The concentrations refer to the model compounds. The *n* stands for the chain length, in atom units. For the convenience of presentation, the *n* for 1 is arbitrarily set to 0. The compounds were purified by chromatography on silica gel with CH_2Cl_2/NH_3-saturated MeOH as eluent. The synthesis of compound 3 is shown in Scheme I.

Scheme I

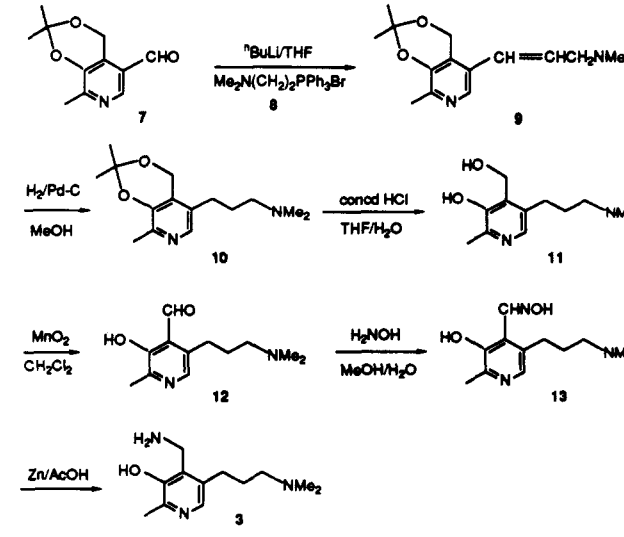

(1) (a) Breslow, R.; Czarnik, A. W.; Laurer, M.; Leppkes, R.; Winkler, J.; Zimmerman, S. *J. Am. Chem. Soc.* **1986**, *108*, 1969 and references therein. (b) Breslow, R.; Chmielewski, J.; Foley, D.; Johnson, B.; Kumabe, N.; Varney, M.; Mehra, R. *Tetrahedron* **1988**, *44*, 5515. (c) Murakami, Y.; Kikuchi, J.; Shiratori, N. *Bull. Chem. Soc. Jpn.* **1989**, *62*, 2045. (d) Ando, M.; Watanabe, J.; Kuzuhara, H. *Bull. Chem. Soc. Jpn.* **1990**, *63*, 88. (e) Ando, M.; Kuzuhara, H. *Bull. Chem. Soc. Jpn.* **1989**, *62*, 244.

(2) Weiner, W.; Winkler, J.; Zimmerman, S. C.; Czarnik, A. W.; Breslow, R. *J. Am. Chem. Soc.* **1985**, *107*, 4093.

(3) Zimmerman, S. C.; Czarnik, A. W.; Breslow, R. *J. Am. Chem. Soc.* **1983**, *105*, 1694.

(4) The previous conclusion (ref 1a) was based mainly on the higher transamination rate with 5 (compared with 4), the stereoselectivity difference associated with chiral side arms, and the rate reversal of transamination rates vs elimination rates. However, without the evidence that the rate with 3 ($n = 3$) is higher than with 4 ($n = 4$), the interpretation that higher rate with 5 ($n = 5$) is due to faster intramolecular reprotonation rather than deprotonation is much less convincing. Also, this interpretation cannot explain the rate (ref 18) of 3.8×10^{-4} (at 0.16 mM) with another compound ($n = 2$). The stereoselectivity is not conclusive evidence for the dual function either; it might be a consequence of asymmetric deprotonation—before the chiral side arm moves out after deprotonation from the C-4 methylene group, some other species in the solution reprotonates the α-carbon of the developing amino acid from the other face. As for the comparison of transamination rates and elimination rates, since the two sets of rates were determined in two different reaction systems, the conclusion must be treated with additional caution.

(5) For further details, see: Wu, Y. Ph.D. Dissertation, University of Göteborg, Göteborg, Sweden, 1991.

(6) At concentrations much higher than 0.32 mM the salt effect is predicted to be too large and therefore may mask the rate–structure dependence, while at concentrations much lower than 0.08 mM, the experimental errors may be too large.

(7) Unlike in the previous work (ref 1a), where the crude compounds (containing unspecified amounts of NaBr) were directly used in kinetic experiments, all model compounds in the present study were purified by chromatography on silica gel (with CH_2Cl_2/NH_3-saturated MeOH as eluent).

0022-3263/92/1957-6324$03.00/0 © 1992 American Chemical Society

Table II.[a] The Influence of Ionic Strength on the k_{obsd} in the Transamination System with 5

KBr	0 mM	0.48 mM	1.6 mM
k_{obsd}/s^{-1}	6.7×10^{-4}	6.1×10^{-4}	5.1×10^{-4}

[a] All runs were carried out in MeOH at "pH 4.0" (as read with a glass electrode) at 30.0 °C with 0.16 mM of 5, 1.6 mM of pyruvic acid, 0.16 mM of $Zn(OAc)_2 \cdot 2H_2O$, plus the indicated amount of KBr. The standard deviations were <1% with duplicate runs within 10%.

Based on the values of the relative rates (k_b/k_a or k_c/k_a), the compounds can be divided into two groups; one ($n < 4$) shows significant rate increase (k_b/k_a and $k_c/k_a > 1$) with the increase of reactant concentration while the other ($n \geq 4$) essentially does not. This indicates that the intramolecular mechanism predominates in the transamination systems with the latter group of compounds (i.e., the side arm base conducts both deprotonation and reprotonation in the ketimine–aldimine tautomerization).

From molecular models it can be seen that to deliver a proton intramolecularly to the α-carbon of the developing amino acid the chain length between the pyridine ring and the NMe_2 must be four atom units (still with some conformational disadvantage) or longer. This explains why those with shorter chains fail to show intramolecularity.

The rate decreases (i.e. $k_c < k_b < k_a$) with 5 and 6 are most likely caused by the concomitant change in the ionic strength (salt effect) when the reactant concentrations increase. Similar rate decreases were indeed observed by adding KBr to the transamination system with 5 (Table II). Since the salt effect is expected to occur with all other model compounds, with respect to the given concentration increase the "total" increase in the k_{obsd} should be larger than observed: $\delta' k_{obsd} = \delta k_{obsd} + RD$, where δk_{obsd} is the observed k_{obsd} increase (e.g., $k_b - k_a$, when concentration increases from 0.08 to 0.16 mM) and RD (>0) is the rate depression[8] due to the salt effect. Although experimentally the RD is indeterminable, its variation is expected to be well within limits[9] that the $\delta' k_{obsd}$ vs n curve still retains the same shape as corresponding δk_{obsd} vs n curve (Figure 3), with a peak at $n = 3$ and a valley at $n = 5$. On one hand, this assumption is justified by the striking structural resemblance of the model compounds (they carry the same number of positive charges at pH 4) and the relatively low

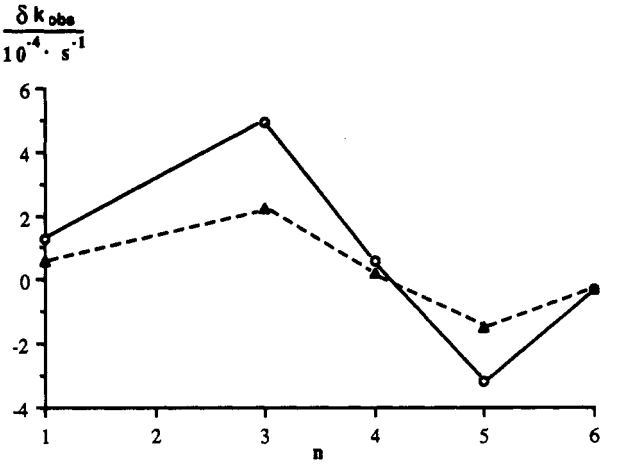

Figure 3. The plots of δk_{obsd} vs n, where $\delta k_{obsd} = k_0 - k_a$ (open circles) or $k_b - k_a$ (triangels). The k_a, k_b and k_c data are taken from Table I.

proportion of the model compound in the reaction system. On the other hand, any alternative to this assumption requires that the RD varies in an unreasonable way; with $n = 3$ it must be smaller than those with $n = 1$ and $n = 4$, while with $n = 5$ it must be larger than those with $n = 4$ and $n = 6$. Thus, despite the indeterminability of the RD, the conclusion that 5 shows much higher intramolecularity than those with shorter side arms is not affected.

For the compound without any access to the intramolecular paths ($n = 0$), both the deprotonation and the reprotonation must be fulfilled intermolecularly. As a consequence, the k_{obsd} is expected to show a linear dependence on the concentration of model compound. Indeed, at low concentrations when the salt effect is not strong enough to interfere, the k_{obsd} is essentially proportional to the concentration of the model compound.

It is interesting to note that compound 4 shows higher intramolecularity but lower rates (k_{obsd}'s) than 3. This means that the intramolecular deprotonation with the latter is very efficient,[10] which fully makes up for the disadvantage of lacking an intramolecular reprotonation path. Hence, $n = 3$ must be the optimum length[11] for the intramolecular deprotonation.

Longer chains have more degrees of freedom, which decrease the probability for the side arm base to reach the appropriate conformation to carry out intramolecular deprotonation. Thus, extension of the side chain from four to five atom units is expected to result in even lower intramolecular deprotonation rates and consequently, lower overall rates (k_{obsd}'s). Interestingly, compound 5 ($n = 5$) shows higher rates at the two lower concentrations.[12] Since in this case the intramolecular mechanism predominates as shown by the relative rates (k_b/k_a and k_c/k_a), the higher overall rates must be due to a fast intramolecular reprotonation.

(8) For a given concentration, the ionic strength is essentially decided by the number of the charges carried by the species, which is highly likely to be the same for the closely related compounds as used in the present work. Consequently, the RD is also more or less the same with those compounds. The correctness of the conclusion, however, does not entirely rely on this assumption (constant RD).

(9) The smallest $\delta' k_{obsd}$ ($= \delta k_{obsd} + RD$) does not necessarily mean the smallest relative rate $((k_b + RD)/k_a$ and/or smallest $(k_c + RD)/k_a)$ after calibration for the salt effect. In the present case, however, at least at up to 0.16 mM it can be proven that the smallest $\delta' k_{obsd}$ corresponds to the smallest k_b/k_a. Based on the assumption that the smallest $\delta' k_{obsd}$ occurs at $n = 5$, we obtain $(k_b)_5 - (k_a)_5 + (RD)_5 < (k_b)_x - (k_a)_x + (RD)_x$, where $(k_a)_5$ and $(k_b)_5$ are the k_{obsd} with 5 ($n = 5$) at the two concentrations while $(k_a)_x$ and $(k_b)_x$ are the k_{obsd}'s with another compound ($n = x \neq 5$). Dividing the both sides of the inequality by $(k_a)_5$ gives

$$((k_b)_5 - (k_a)_5 + (RD)_5)/(k_a)_5 < ((k_b)_x - (k_a)_x + (RD)_x)/(k_a)_5$$

Since $(k_a)_5 > (k_a)_x$, it follows that

$$((k_b)_5 - (k_a)_5 + (RD)_5)/(k_a)_5 < ((k_b)_x - (k_a)_x + (RD)_x)/(k_a)_x$$

or

$$[((k_b)_5 + (RD)_5)/(k_a)_5] - 1 < [((k_b)_x + (RD)_x)/(k_a)_x] - 1$$

Therefore, $((k_b)_5 + (RD)_5)/(k_a)_5 < ((k_b)_x + (RD)_x)/(k_a)_x$, which means after calibration for the salt effect, 5 still shows the smaller relative rate (higher intramolecularity) than other compounds.

(10) Another alternative that the high overall rate (k_{obsd}) with 3 is caused by high intermolecular deprotonation and/or reprotonation rates does not seem to be possible. If, because of its shorter side arm, 3 ($n = 3$) gave higher intermolecular rates than 4 ($n = 4$), the compounds with $n = 1$ or 2 would give higher overall rates than 3.

(11) This is in full consistence with the optimum ring size (eight-membered ring) found in other comparable intramolecular deprotonation systems. See: Hine, J. *Acc. Chem. Res.* **1978**, *11*, 1.

(12) At 0.32 mM, the rate with 5 is lower than that with 3. This is because the rate acceleration gained by creating an additional intramolecular reprotonation path does not increase with the increase of the reactant concentration. The k_{obsd} for intermolecular paths, however, does increase. When the concentration reaches certain level, the rate reversal is of course unavoidable. Similar rate reversal is also found between 2 and 6.

In summary, by varying reactant concentrations we have obtained further evidence to support the conclusion form the previous study[1a,2,3] that a basic side arm in pyridoxamine derivatives plays a dual function, with $n = 5$ as the optimum chain length. Moreover, by introducing a new compound with $n = 3$, we demonstrate that this optimum length ($n = 5$) is due to its highly efficient intramolecular reprotonation that fully compensates its less efficient intramolecular deprotonation. The most favorable chain length for the intramolecular deprotonation is three atom units. When the side chain is long enough to reach the α-carbon of the developing amino acid, both the deprotonation and the reprotonation are accomplished intramolecularly. The highest intramolecularity occurs in the compound with a side chain of five atom units.

Experimental Section

General. Hydroxylamine hydrochloride (99%), ^{n}BuLi (2.5M), pyruvid acid (98%), and Pd–C (5%) were purchased from Aldrich. Compound 8 [(2-(dimethylamino)ethyl)triphenylphosphonium bromide], $Zn(OAc)_2 \cdot 2H_2O$ (99%), activated MnO_2 (90%), and Zn powder (98%) were purchased from Fluka. The MeOH–NH_3 used in the column chromatography (on 230–400-mesh silica gel) was obtained by bubbling gaseous NH_3 into MeOH at 0 °C for ca. 1 h. ^{1}H and ^{13}C NMR spectra were recorded at either 400 or 500 MHz for ^{1}H with Me_4Si as the internal standard and [$^2H_1$]-chloroform as the solvent unless otherwise specified. Mass spectra (GC/MS) were obtained with electron impact ionization (70 eV). The relative intensity of each peak is given in parentheses after the corresponding m/e value. Elemental analyses were carried out by Microkemi AB, Uppsala, Sweden.

All kinetic experiments were carried out in the same way[13] under the same conditions, with a constant molar ratio[14] of 1:10:1 of model compound/pyruvic acid/$Zn(OAc)_2 \cdot 2H_2O$. Stock solutions of the reactants were freshly prepared from corresponding compounds and deaerated MeOH. For each particular run the required amounts of stock solutions were mixed together and further diluted with deaerated MeOH to such a level that after adjusting the acidity with 0.012 mM methanolic HCl to pH 4.00 ± 0.01 (as read with a glass electrode) the total volume was exactly as required. The mixture was then transferred to a UV cuvette, and the reaction was followed at 385 nm. The cuvette holder was thermostated at 30.00 ± 0.05 °C throughout the whole reaction period. The aldimine–Zn^{2+} absorbance (385 nm) was recorded at regular intervals until it started decreasing[15] constantly.

5-[3-(Dimethylamino)-1-propenyl]-2,2,8-trimethyl-4*H*-1,3-dioxino[4,5-*c*]pyridine (9). With cooling (ice bath) and stirring, 3.2 mL of ^{n}BuLi (ca. 2.3 M) was added (via a syringe) over 12 min to a stirred solution of 8 (2.857 g, 6.9 mmol) in dry THF (20 mL) under nitrogen. After completion of addition the orange mixture was stirred for another 50 min before a solution of 7[16] (1.429 g, 6.9 mmol) in dry THF (5 mL) was introduced via a syringe over 5 min. The dark brown mixture was stirred for 3.5 h during which the orange color appeared again. The reaction mixture was partitioned between diethyl ether and water. The ethereal phase was washed with brine (until the aqueous phase became neutral) and dried over anhydrous Na_2SO_4. After filtration and evaporation the residue was chromatographed (2:1 followed by 1:1 of CH_2Cl_2/MeOH) to yield *cis*-**9** (509 mg) [^{1}H NMR δ 7.86 (s, 1 H), 6.32 (br d, J = 11.4 Hz, 1 H), 5.94 (dt, J = 11.6, 6.6 Hz, 1 H), 4.70 (s, 2 H), 3.06 (dd, J = 1.8, 6.6 Hz, 2 H), 2.42 (s, 3 H), 2.20 (s, 6 H), 1.55 (s, 6 H); ^{13}C NMR δ 146.54, 145.64, 139.71, 133.44, 126.45, 124.55, 123.62, 99.68, 59.07, 57.09, 45.29, 24.66, 18.47; MS m/e 262 (M^+, 5.67), 204 (28.8), 159 (56.9), 91 (62.5), 71 (100), 58 (86.7)] and (2:1 of CH_2Cl_2/MeOH–NH_3) *trans*-**9** (452 mg): ^{1}H NMR δ 8.12 (s, 1 H), 6.32 (br d, J = 16.0 Hz, 1 H), 6.15 (dt, J = 15.8, 6.5 Hz, 1 H), 4.83 (s, 2 H), 3.08 (dd, J = 1.1, 6.4 Hz, 2 H), 2.39 (s, 3 H), 2.24 (s, 6 H), 1.55 (s, 6 H); ^{13}C NMR δ 146.45, 145.51, 137.83, 131.48, 126.91, 125.24, 123.42, 99.44, 62.10, 59.19, 45.26, 24.66, 18.45; MS m/e 262 (M^+, 6.88), 204 (25.6), 160 (40.8), 91 (42.2), 71 (99.5), 58 (100). Anal. Calcd for $C_{15}H_{22}N_2O_2$: C, 68.67; H, 8.45; N, 10.68. Found: C, 68.4; H, 8.5; N, 10.1.

5-[3-(Dimethylamino)propyl]-2,2,8-trimethyl-4*H*-1,3-dioxino[4,5-*c*]pyridine (10). A mixture of *cis*-**9** (349 mg, 1.33 mmol) and 5% Pd/C (227 mg) in MeOH (10mL) was stirred at room temperature under H_2 (balloon) for 4 h, when GC/MS showed full consumption of the starting material. The solid was filtered off, and the filtrate was concentrated on a rotary evaporator. The residue was chromatographed on silica gel (2:1 of CH_2Cl_2/MeOH followed by 20:3 of CH_2Cl_2/MeOH–NH_3) to give **10** as a gum (251 mg, 95%): ^{1}H NMR δ 7.88 (s, 1 H), 4.82 (s, 2 H), 2.46 (t, J = 7.8 Hz, 2 H), 2.38 (s, 3 H), 2.30 (t, J = 7.3 Hz, 2 H), 2.23 (s, 6 H), 1.73 (br quintet, 2 H), 1.54 (s, 6 H); ^{13}C NMR δ 145.68, 145.40, 139.96, 130.28, 124.79, 99.36, 58.92, 58.76, 45.39, 27.82, 26.51, 24.68, 18.30; MS m/e 264 (M^+, 10.2), 204 (2.5), 191 (8.8), 91 (5.4), 71 (18.3), 58 (100).

5-[3-(Dimethylamino)propyl]-4-(hydroxymethyl)-2-methyl-3-pyridinol (11). A mixture of **10** (218 mg, 0.82 mmol), THF (10 mL), H_2O (6 mL), and 37% HCl (4 mL) was stirred at room temperature for 24 h. Most of the solvent was removed on a rotary evaporator, and the residue was coevaporated twice with EtOH to give a yellowish oil. After neutralized with MeOH–NH_3 the crude product was chromatographed on silica gel (5:1 of CH_2Cl_2/MeOH–NH_3) to yield pure **11** as a gum (175 mg, 95%): IR (film) 3094 (br) cm^{-1}; ^{1}H NMR δ 7.73 (s, 1 H), 4.85 (s, 2 H), 2.50 (t, J = 7.6 Hz, 2 H), 2.41 (s, 3 H), 2.26 (t, J = 7.4 Hz, 2 H), 2.18 (s, 6 H), 1.65 (br quintet, J = 7.4 Hz, 2 H); ^{13}C NMR δ 151.23, 145.44, 139.97, 131.74, 130.44, 59.16, 58.26, 44.96, 28.20, 26.80, 18.51; MS m/e 224 (M^+, 2.2), 91 (1.67), 58 (100). Anal. Calcd for $C_{12}H_{20}N_2O_2$: C, 64.26; H, 8.99; N, 12.49. Found: C, 63.9; H, 9.2; N, 12.3.

5-[3-(Dimethylamino)propyl]-3-hydroxy-2-methyl-4-pyridinecarboxaldehyde Oxime (13). A mixture of **11** (89 mg, 0.4 mmol) and activated MnO_2 (400 mg) in CH_2Cl_2 (3 mL) was stirred at room temperature for 2.5 h when TLC showed the completion of oxidation. The solid was filtered off, and the filtrate was concentrated to give crude **12** (71 mg, 80%) as a dark brown oil: IR (film) 3252 (br), 1668 cm^{-1}; ^{1}H NMR δ 11.50 (br s, 1 H), 10.35 (s, 1 H), 7.99 (s, 1 H), 2.95 (t, J = 7.3 Hz, 2 H), 2.51 (s, 3 H), 2.25 (t, J = 6.8 Hz, 2 H), 2.15 (s, 6 H), 1.79 (br quintet, 2 H); MS m/e 222 (M^+, 0.3), 58 (100). To the crude aldehyde were added 3 mL of MeOH, 0.5 mL of H_2O, 70 mg of NaOAc, and 33 mg of $NH_2OH \cdot HCl$. The mixture was stirred at room temperature for 1.5 h, when TLC showed full consumption of the aldehyde. Solvents were removed on a rotary evaporator, and the residue was chromatographed (5:1 of CH_2Cl_2/MeOH–NH_3) to give 64 mg (0.27 mmol, 90%) of **13** as a white solid: IR (film) 3553–2018 (br), 1773 cm^{-1}; ^{1}H NMR δ 10.65 (s, 1 H), 8.45 (s, 1 H), 7.82 (s, 1 H), 2.69 (t, J = 7.8 Hz, 2 H), 2.46 (s, 3 H), 2.44 (t, J = 7.9 Hz, 2 H), 2.36 (s, 6 H), 1.84 (br quintet, J = 7.9 Hz, 2 H); ^{13}C NMR ([$^2H_4$]methanol) δ 152.54, 148.54, 147.00, 140.25, 134.99, 122.02, 59.79, 45.49, 30.35, 28.19, 18.37. Anal. Calcd for $C_{12}H_{19}N_3O_2$: C, 60.74; H, 8.07; N, 17.71. Found: C, 60.4; H, 8.2; N, 17.4.

(13) For the protocol of the experimental method, see refs 1a and 19.

(14) The effects of concentrations of α-keto acid and $Zn(OAc)_2$ on the transamination rate with pyridoxamine have been studied by Martell et al.[19] The maximum rate was found with a 1:10:1 (molar) ratio of the reactants. Changing the model compound concentration while still keeping a constant 1:10:1 ratio will inevitably lead to the changes in the concentrations of pyruvic acid and $Zn(OAc)_2$. Fortunately, these do not cause so much complication as one might expect. On one hand, this is because that the general catalysis by the species such as pyruvate and acetate is insignificant (if compared to that by the nitrogen bases in the model compounds)—otherwise, no remarkable changes in the rates should have been observed by only replacing one model compound with another. On the other hand, even if the changes in the concentrations of these species (other than model compound) do cause some effects, whatever they are, they must be the same (if not negligible) for a given concentration change regardless of the model compound. Thus, when the concentrations are changed, e.g., from 0.08 to 0.32 mM, the k_c/k_s for **3** is 2.40 while that for **5** is 0.61. The only possible reason is the structural difference between **3** and **5**, since the rest are exactly the same in both systems.

(15) This is presumably caused by hydrolysis/methanolysis. In plots of absorbance vs time it appears as slight drops off the first-order curves (occurred in the flat regions of the curves, far less than 1% of the maximum absorbance) and has not been taken into the calculations. The same treatment has been used in the previous studies (refs 1, 3, 19).

(16) Wu, Y.; Ahlberg, P. *Acta Chem. Scand.* **1992**, *46*, 60 and the references therein.

4-(Aminomethyl)-5-[3-(dimethylamino)propyl]-2-methyl-3-pyridinol (3). At room temperature with stirring Zn dust (74 mg) was added to a solution of **13** (44 mg, 0.185 mmol) in glacial acetic acid (2 mL). Stirring was continued for another 15 min. The reaction mixture was then filtered through a sintered-glass filter under nitrogen pressure. The filtrate was concentrated on a rotary evaporator and the residue was chromatographed (5:1 followed by 10:3 of CH_2Cl_2/MeOH–NH_3) to afford 37 mg (0.166 mmol) of **3** as an off-white solid:[17] ^1H NMR ([$^2H_4$]methanol) δ 7.55 (s, 1 H), 4.10 (s, 2 H), 2.58 (t, J = 7.8 Hz, 2 H), 2.39 (t, J = 7.7 Hz, 2 H), 2.33 (s, 3 H), 2.27 (s, 6 H), 1.70 (br quintet, J = 7.8 Hz, 2 H); ^{13}C NMR ([$^2H_4$]methanol, with the central line of the solvent heptet set to 49.0 ppm as ref) δ 146.15, 136.85, 134.79, 130.81, 125.36, 59.32, 44.77, 39.54, 28.68, 28.18, 18.04.

Acknowledgment. We thank the Swedish Natural Science Research Council for support.

Registry No. **1**, 85-87-0; **2**, 96825-29-5; **3**, 143732-82-5; **4**, 96806-37-0; **5**, 96806-38-1; **6**, 101348-88-3; **7**, 6560-65-2; **8**, 21331-80-6; *cis*-**9**, 143732-83-6; *trans*-**9**, 143732-83-6; **10**, 143732-84-7; **11**, 143732-85-8; **12**, 143732-86-9; **13**, 143732-87-0; pyruvic acid, 127-17-3; transaminase, 9031-66-7.

(17) This solid is quite air-sensitive, which turns yellow in seconds on contact with air. As expected, the NMR spectra are concentration/pH-dependent.
(18) Chmielewski, J. Ph.D. Dissertation, Columbia University, 1988.
(19) Matsushima, Y.; Martell, A. *J. Am. Chem. Soc.* **1967**, *89*, 1331.

11-Hydroxystaurosporine: A Highly Cytotoxic, Powerful Protein Kinase C Inhibitor from a Tunicate

Robin B. Kinnel[1] and Paul J. Scheuer*

Department of Chemistry, University of Hawaii at Manoa, 2545 The Mall, Honolulu, Hawaii 96822

Received May 11, 1992

Ascidians, the largest class in the subphylum urochordata (tunicates), are highly developed sessile animals often rich in bioactive secondary metabolites.[2] Noteworthy examples are the didemnins, depsipeptides that show considerable promise as antitumor agents,[3] the antiviral β-carbolines such as the eudistomins,[4] cytotoxic iminoquinone pigments like wakayin[5] and the discorhabdins,[6] and the pentacyclic alkaloid shermilamine.[7] The indolo[2,3-*a*]carbazole ring system is not represented among alkaloids isolated from marine sources, although numerous indolocarbazoles are known from terrestrial microorganisms, slime molds,[8] and more recently, from fresh water blue-green algae.[9] We report here the isolation and structure proof of 11-hydroxystaurosporine (**2**), the first indolo[2,3-*a*]carbazole to be isolated from a marine organism. A dihydroxy derivative, 3,11-dihydroxystaurosporine (**3**), was also isolated but was incompletely characterized due to lack of material. Both are active against human nasopharyngeal cancer cells, and **2** is more potent than staurosporine (**1**) in protein kinase C (PKC) inhibition.

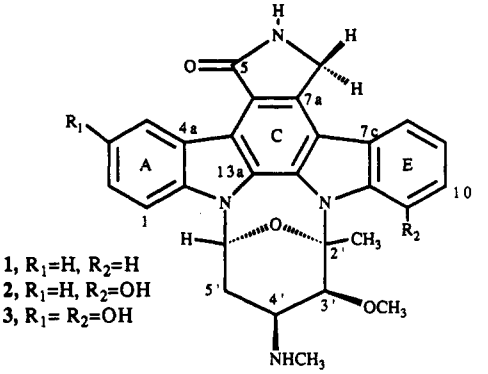

A brown tunicate, *Eudistoma* sp. (family Polycitoridae) was collected in June 1990 in Sapwale Bay, Pohnpei (Federated States of Micronesia), by snorkeling at −1 to −2 m. It was frozen and then lyophilized. Assays of both lipophilic and hydrophilic extracts revealed potent cytotoxic activity, which suggested either a number of active metabolites or a few compounds of intermediate polarity. Extraction of the freeze-dried animal with methanol, followed by solvent partition, then silica gel and RP-18 flash chromatography, and finally HPLC afforded 3.4 mg (0.013%) of **2** as a pale yellow amorphous solid, which discolored slowly in contact with air.

The UV spectrum suggested an extended aromatic chromophore. Since it was unaffected by the addition of acid but underwent reversible bathochromic–hyperchromic shifts of the maxima at 248 and 254 nm (but not those at 292 and 300 nm) upon addition of base, a phenol is likely present.

A combination of ^{13}C NMR spectroscopy and high-resolution, fast atom bombardment mass spectrometry (HRFABMS) established a molecular formula of $C_{28}H_{26}N_4O_4$. The ^1H NMR spectrum revealed the presence of seven aromatic protons, including a very low field doublet at 9.24 ppm. These protons were on two rings, 1,2-di- and 1,2,3-trisubstituted. ^{13}C NMR resonances were observed for 18 aromatic carbons, one carbonyl, and nine other carbons. Most striking were the three resonances between 82 and 100 ppm, which at first suggested the presence of acetylenic, carbinolamine or acetal carbons.

A literature search uncovered two compounds with the same composition, UCN-01 and UCN-02, epimeric 7-hydroxy derivatives of staurosporine.[10] Comparison of ^{13}C and ^1H NMR spectra and the UV spectrum of staurosporine with those of **2** revealed that the two compounds were very similar. Staurosporine (**1**) has the molecular formula $C_{28}H_{26}O_3N_4$; hence **2** has one more oxygen. Since there is no proton at C-11, but there is an exchangeable proton, the phenolic group must be present at that position. Comparison of the calculated ^{13}C and ^1H chemical shifts in ring E (using staurosporine as the model) with those observed in **2** reveals excellent agreement. In addition, **2** forms a diacetate, which provides chemical evi-

(1) On leave from Hamilton College, Clinton, NY 13323.
(2) For reviews, see: Faulkner, D. J. *Nat. Prod. Rep.* **1991**, *8*, 97–147 and earlier reviews.
(3) Rinehart, K. L.; Gloer, J. B.; Cook, J. C., Jr. *J. Am. Chem. Soc.* **1981**, *103*, 1857–1859.
(4) Rinehart, K. L.; Kobayashi, J.; Harbour, G. C.; Gilmore, J.; Mascal, M.; Holt, T. G.; Shield, L. S.; Lafargue, F. *J. Am. Chem. Soc.* **1987**, *109*, 3378–3387.
(5) Copp, B. R.; Ireland, C. M.; Barrows, L. R. *J. Org. Chem.* **1991**, *56*, 4596–4597.
(6) Perry, N. B.; Blunt, J. W.; Munro, M. H. G.; Higa, T.; Sakai, R. *J. Org. Chem.* **1988**, *53*, 4127–4128.
(7) Cooray, N. M.; Scheuer, P. J.; Parkanyi, L.; Clardy, J. *J. Org. Chem.* **1988**, *53*, 4619–4620.
(8) For a recent review of indolocarbazoles isolated from natural sources, see: Gribble, G. W.; Berthel, S. In *Studies in Natural Products Chemistry*; Rahman, A., Ed.; Elsevier: New York, in press.
(9) Knubel, G.; Larsen, L. K.; Moore, R. E.; Levine, I. A.; Patterson, G. M. L. *J. Antibiot.* **1990**, *43*, 1236–1239. Bonjouklian, R.; Smitka, T. A.; Doolin, L. E.; Molloy, R. M.; Debono, M.; Shaffer, S. A.; Moore, R. E.; Stewart, J. B.; Patterson, G. M. L. *Tetrahedron* **1991**, *47*, 7739–7750.
(10) Takahashi, I.; Saitoh, Y.; Yoshida, M.; Sano, H.; Nakano, H.; Morimoto, M.; Tamaoki, T. *J. Antibiot.* **1989**, *52*, 571–576. See also: Furusaki, A.; Hashiba, N.; Matsumoto, T.; Hirano, A.; Iwai, Y.; Omura, S. *J. Chem. Soc., Chem. Commun.* **1978**, 800–801.

0022-3263/92/1957-6327$03.00/0 © 1992 American Chemical Society